



ISSN: 2230-9926

Available online at <http://www.journalijdr.com>

IJDR

International Journal of Development Research

Vol. 12, Issue, 04, pp. 55519-55526, April, 2022

<https://doi.org/10.37118/ijdr.24286.04.2022>



RESEARCH ARTICLE

OPEN ACCESS

ANALYTICAL AND EXPERIMENTAL EVALUATION OF A HOUSEHOLD REFRIGERATOR OPERATING UNDER A DIFFUSION-ABSORPTION REFRIGERATION CYCLE

Túlio Tito Godinho de Rezende¹, Flávio Neves Teixeira^{1,*}, José Antônio da Silva¹, Luiz Gustavo Monteiro Guimarães¹, Matheus dos Santos Guzella² and Osvaldo José Venturini³

¹Federal University of São João del Rei, Campus CSA, Praça Frei Orlando 170, 36.307-352, São João del Rei, Minas Gerais, Brazil; ²Federal University of Vales do Jequitinhonha e Mucuri, Campus JK, Rodovia MGT 367 - Km 583, 39100-000, Diamantina, Minas Gerais, Brazil; ³Federal University of Itajubá, Av BPS 1303, Pinheirinho, 37500-903, Itajubá, Minas Gerais, Brazil

ARTICLE INFO

Article History:

Received 10th January, 2022

Received in revised form

19th February, 2022

Accepted 14th March, 2022

Published online 30th April, 2022

Key Words:

Absorption machine, Diffusion-absorption refrigeration cycle; Analytical and experimental Investigation; COP.

*Corresponding author:

Túlio Tito Godinho de Rezende,

ABSTRACT

The diffusion-absorption refrigeration (DAR) cycle has characteristics as the use of three working fluids and a low COP. In this work, an analytical and experimental investigation of a household refrigerator operating under a H₂O-NH₃-H₂DAR cycle is performed. A thermodynamic model of the DAR cycle was developed and adjusted based on models available in the literature. An experimental investigation was performed aiming to validate the developed DAR model using operating data collected in a real refrigerator. Subsequently the role of refrigerant rectification in the cycle was investigated and it was found that the temperature at the outlet of the rectifier should not exceed 70 °C. In addition, the importance of the production of liquid refrigerant in the condenser was investigated. It was observed that the COP decreases with the increase in the temperature of the inert gas entering the liquid heat exchanger (LHE). Finally, it was demonstrated that by increasing the amount of inert gas in the evaporator, there is a drop in evaporation temperature and consequently in the system COP. The model proved to be robust in the operational conditions tested experimentally.

Copyright©2022, Beatriz Marciel et al. This is an open access article distributed under the Creative Commons Attribution License, which permits unrestricted use, distribution, and reproduction in any medium, provided the original work is properly cited.

Citation: Túlio Tito Godinho de Rezende, Flávio Neves Teixeira, José Antônio da Silva, Luiz Gustavo Monteiro Guimarães, Matheus dos Santos Guzella and Osvaldo José Venturini. "Analytical and experimental evaluation of a household refrigerator operating under a diffusion-absorption refrigeration cycle", *International Journal of Development Research*, 12, (04), 55519-55526.

INTRODUCTION

Two Swedish engineers, Von Platen and Munters (1928), designed the diffusion-absorption refrigeration (DAR) cycle. It has a unique characteristic when compared to other conventional refrigeration cycles: operation with three working fluids (ammonia refrigerant, water as a transport fluid and an inert gas, usually hydrogen or helium). The function of the inert gas is to reduce the partial pressure of the refrigerant in the evaporator, allowing it to evaporate at lower temperatures and, consequently, producing the refrigeration effect. This cycle operates under a constant pressure and the refrigeration circulation is obtained through a bubble pump (internal tube of the generator). It only requires a heat source to operate and, by having no moving parts, it is reliable and quiet. All these characteristics make the system compact and easy to manufacture, but with a very low COP in comparison to other refrigeration cycles. Several studies aiming to increase the efficiency of the DAR cycle are being developed focusing on a better understanding its processes and

behavior. Chen et al. (1996) redesigned the generator, in order to include a heat exchanger that reuses the heat from the weak solution, returning from the separator, to the preheat the strong solution entering the generator, leading to a 50% increase in the system COP. Sriksirin and Aphornratana (2002) developed a mathematical model in order to describe the DAR cycle operating with helium as inert gas. The authors performed an experiment with air and water to determine the bubble-pump performance. When comparing the numerical results with the experiment data, it was found that the system performance had a strong dependence of the bubble-pump characteristics, in addition to the absorber and evaporator mass transfer performances. Regarding the modeling of the DAR cycle, Zohar et al. (2005) developed a model for a system operating with ammonia-water-hydrogen and, subsequently, helium as an inert gas. The authors considered the effect of the subcooling at the outlet of the condenser and the presence of an internal heat exchanger. They concluded that the ideal mass fraction of ammonia in the strong solution entering the generator was within the range was 0.2 to 0.3. These authors recommended a mass fraction of ammonia equal to 0.1 for the weak

solution leaving the separator. Starace and De Pascalis (2013) improved the Zohar et al. (2009) model by taking into account the water that escapes along with the ammonia and enters the condenser. The effect over the results showed differences between the predictions of the two models from 2.0% of COP to 8.5% of molar concentration of ammonia in the weak liquid solution. Other studies focused on the investigation of the behavior of the DAR cycle through heat transfer analysis. Mazouzet et al (2014) used a steady-state method and the dynamic method to evaluate the characteristics of a refrigeration system operating under the DAR cycle. As a result, they obtained all the main heat transfer characteristics of the system, especially the global heat transfer coefficients. Mansouri et al (2015) collected data experimentally and used this data as input data in a theoretical simulation model using the Aspen-Plus software. The results were validated by comparing the model's predictions with the experimental data. They concluded that the best performance is experimentally obtained with an input power of 46 W at a generator temperature of 167 °C. Jelinek et al. (2016) investigated different configurations to obtain a determined subcooling degree at the condenser outlet: no subcooling, partial subcooling, and full subcooling. The authors reported that, for the same heat input, the partial subcooling configuration resulted in the highest refrigeration effect and hence, the highest COP. Adjibade et al (2017) experimentally compared two energy sources for the DAR cycle: electrical energy from the grid and heat exchange with exhaust gas from an internal combustion engine. They used heat transfer analysis associated with thermodynamic balances to understand the behavior of each component. The temperature required for operation varied between 140 °C and 152 °C for gas and electrical sources, respectively. They concluded that it is possible to use exhaust gases as an energy source for the DAR cycle.

Mansouri et al (2017) investigated experimentally a low capacity commercial DAR refrigerator during transients (dynamic operation) and used the collected experimental data to determine global heat transfer coefficients of the system components. They performed tests imposing different powers on the electrical resistance of the generator. With the data obtained, they developed a dynamic model called black box. They found that a minimum power of 35 W is necessary for the cycle to operate with stability. When comparing the model with the experimental data, they verified a maximum relative deviation of 8.2% (between the predicted values by the model and the experimental data) and the maximum relative deviation in COP prediction is about 8.0%. Saâfi, et al (2019) studied the behavior of the DAR cycle under different operating conditions and evaluated its performance. A DAR machine was equipped 18 thermocouples type K fixed by clamps on the outer surfaces of the tubes at specific positions, each one representing a cycle state. A series of tests were carried out, varying the generator power from 15 W to 63 W. They verified that a minimum of 23 W of power is necessary to guarantee the production of cold.

They concluded, through analysis of the different conditions that the studied machine reaches a maximum COP of 0.15 under 43 W of power in the generator. One of the major difficulties when analyzing a DAR cycle is the calculation of the mass flow rate. Most of the authors compute this quantity considering a mass balance in the generator. In this case, the mass fraction of ammonia in the ammonia-water solution should be known. When the concentration of the solution is unknown, the results might lose their accuracy. Rezende et al. (2020), proposed a mathematical model to compute the ammonia mass flow rate based only on the inlet and outlet temperatures and the geometric parameters of the condenser. Using experimental data collected in-situ using a thermographic camera, and solving a set of equations using the Engineering Equation Solver (EES®) software the mass flow rate can then be determined. This article aims to apply a thermodynamic model of the DAR cycle and using data experimentally collected in a domestic refrigerator, to evaluate its accuracy. The model can be used as a tool to assess cycle behavior and characteristics.

MATERIALS AND METHODS

DAR system description: Its operation (Fig. 1) can be explained as follows, by starting with the reservoir: the strong liquid solution leaves the reservoir (11) and follows, by gravity, to the LHE, where the solution absorbs part of the heat from the weak solution returning from the generator (2), the strong solution absorbs heat from any available heat source (Q_G) and vapor bubbles are formed inside the tube. Due to the difference in the specific volume, the bubbles begin to rise along the tube, carrying the liquid solution that has not evaporated to the top of the generator.

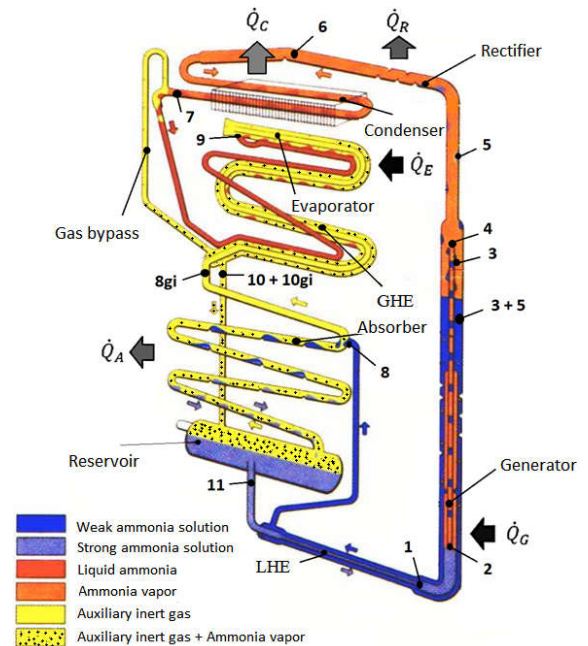


Fig. 1. Schematic view of a DAR system - Adapted from Santner (2009)

The strong solution enters the rectifier (4), while the remaining weak solution (3) enters the absorber, due to the pressure difference. The weak solution transfers heat to the strong solution in the liquid heat exchanger. The weak solution returns to the top of the absorber (8), flowing through the tubes. Meanwhile, it absorbs the ammonia from the hydrogen gas, which takes the reverse path, until it reaches the reservoir. At the top of the generator, the strong solution enters the rectifier (5), where the remaining water will condensate. In the condenser, the ammonia reaches its saturation temperature (7), due to heat transfer to the environment. A by-pass tube is required to ensure that excess ammonia vapor can escape into the reservoir. The liquid ammonia from the condenser flows through a tube with a smaller section. In addition, effects of heat transfer from the sub-cooled liquid in the gas heat exchanger (GHE) and the evaporator are present. Upon entering the evaporator, liquid ammonia is in contact with almost pure hydrogen. Through the phenomena involving Dalton's law, psychrometric imbalance and diffusion, there will be an ammonia temperature drop. From the evaporator, the mixture of ammonia vapor and hydrogen gas enters the reservoir (10) through the absorber, transferring heat to the weak solution, following in the opposite direction. As follows, ammonia is absorbed by the solution. Upon reaching the gas heat exchanger, there will be almost pure hydrogen, which will transfer heat to the mixture returning from the evaporator. This causes the condensation of the remaining ammonia. The cycle closes when the hydrogen finally reaches the condensed ammonia in the evaporator (9).

Experimental setup: In order to experimentally verify the accuracy of the model developed, a small refrigerator operating under a DAR cycle was considered. The inlet and outlet temperatures of the generator, condenser, and evaporator were measured. The outlet temperature of the absorber reservoir, the inlet temperature of the

weak solution at the top of the absorber and the ambient temperature are also measured. The mixture heating in the generator is carried out by means of an electrical resistor. Based on the Joule's effect the energy dissipation can then be measured. The voltage (U) applied in the resistor was measured and its resistance (Rel), that is fixed value, was obtained. The measurements of the voltage and the resistance were taken with a multimeter with $\pm (1\% + 4D)$ accuracy for AC voltage in the 200 V range with 0.1 V resolution (D) and precision of 1%. For the resistance $\pm (1\% + 3D)$ accuracy for resistance in the 200 Ω range with 0.1 Ω resolution (D). Therefore, the power dissipated by the resistor (Q_G) was calculated from:

$$Q_G = \frac{U^2}{R_{el}} \quad (1)$$

Nine DS18B20 sensors were used, with a reading within the range of -55 °C to 125 °C, with an accuracy of ± 0.5 °C within the range of -10 °C to 85 °C and precision of 0.4%. For the measurement points represented by the points 2, 3 and 4 (3 and 4 are in the same position) shown in Fig. 1, since the temperature reaches values higher than 80 °C, two type K thermocouples with a MAX6675 module were used (precision of 0.2%). These thermocouples operate within the range of 0 °C to 800 °C and accuracy of ± 1.5 °C. The sensors were placed in contact with the outer surface of the tubes and insulated with polyurethane foam for accurate measurements. The sensors were connected to a protoboard and to an Arduino Uno R3 microcontroller that sent the data to a computer. Following the methodology proposed by Holman (2012), the combined uncertainty for the global heat transfer coefficient was found to be 1.1%.

Thermodynamic model: The following simplification assumptions are considered for the development of the thermodynamic model:

- Pressure drop at the tubes and the hydrostatic pressure are disregarded;
- The weak solution (point 3 + 5 of Fig. 1) is not heated by the generator before flowing to the liquid heat exchanger;
- An amount of the heat input on the generator (\dot{Q}_P) is lost to the surroundings;
- Inside the generator, the liquid solution (point 3) and the vapor bubbles (point 4) exit the pump at the same temperature, e. g., $T_4 = T_3$;
- The vapor and gases properties were computed assuming ideal gas behavior;
- At the inlet of the condenser, it was considered a mixture of ammonia and water. This is a more reliable approach for the model;
- At point 7, the refrigerant is assumed to be saturated liquid and there is no by-pass gas;
- Since the air is the external fluid, the outlet temperature of the strong solution leaving the reservoir (point 11) is the same as the refrigerant (point 7), e. g. $T_7 = T_{11}$;
- At the outlet of the GHE (point 10), the refrigerant is saturated vapor;
- There is no absorption inside the reservoir;
- The mixture process between the H_2 and the refrigerant at the inlet of the evaporator (point 9) was assumed adiabatic;
- The weak solution at the inlet of the absorber (point 8) and the strong solution at the inlet of the absorber (point 1) were considered to be under equilibrium;
- The LHE was assumed adiabatic;
- The temperature of the H_2 at the points 9 and 10 is the same as the refrigerant, e. g., $T_{9gi} = T_9$ and $T_{10gi} = T_{10}$.
- The temperature of the H_2 at the inlet of the GHE (point 8gi) is equal to the temperature of the weak solution (point 8) at the inlet of the absorber, e. g. $T_{8gi} = T_8$;

First-principles Equations: The model is based on the mass and energy conservation equations, considering Fig. 1. Each component of the DAR system is analyzed separately.

Generator

The general mass balance equations can be written as:

$$\dot{m}_1 = \dot{m}_2 \quad (2)$$

$$\dot{m}_1 = \dot{m}_3 + \dot{m}_4 \quad (3)$$

The mass balance for the ammonia is expressed as:

$$\dot{m}_1 X_1 = \dot{m}_3 X_3 + \dot{m}_4 X_4 \quad (4)$$

At the generator, the energy balance is:

$$\dot{Q}_P = \dot{m}_3 (h_{3'} - h_3) + \dot{m}_4 (h_{4'} - h_4) \quad (5)$$

The specific enthalpies at the points 3 and 4 refer to the adiabatic condition at the bubble pump: $T_4 = T_3 = T_2$.

The general energy equation can be written as:

$$\dot{Q}_G - \dot{Q}_P = \dot{m}_3 h_{3'} - \dot{m}_1 h_1 + \dot{m}_4 h_{4'} \quad (6)$$

Rectifier

The general equation for the balance is:

$$\dot{m}_4 = \dot{m}_5 + \dot{m}_6 \quad (7)$$

For the refrigerant, the mass balance is:

$$\dot{m}_4 X_4 = \dot{m}_5 X_5 + \dot{m}_6 X_6 \quad (8)$$

The general equation for the energy balance is written as:

$$\dot{Q}_R = \dot{m}_4 h_4 - (\dot{m}_5 h_5 + \dot{m}_6 h_6) \quad (9)$$

Condenser

The energy balance equation is:

$$\dot{Q}_C = \dot{m}_6 (h_6 - h_7) \quad (10)$$

Evaporator and gas heat exchanger (GHE): On the refrigerant side, the following mass balance equations can be written:

$$\dot{m}_6 = \dot{m}_7 \quad (11)$$

$$\dot{m}_7 = \dot{m}_9 \quad (12)$$

$$\dot{m}_9 = \dot{m}_{10} \quad (13)$$

Since the concentration of the refrigerant is constant through the evaporator:

$$X_6 = X_7 = X_9 = X_{10} \quad (14)$$

The calculation of the mass flow rate of the inert gas, Eq. (15), was performed following the hypothesis of ideal gas and that it is at the temperature of the refrigerant at the same points. In addition, it is worth mentioning that the gas constant in the case of the use of hydrogen as an inert gas is that of hydronium, due to the interaction of hydrogen under high pressure with water.

$$\dot{m}_{gi} = \left(\frac{P - P_9}{P_9} \right) \left(\frac{X_6 R_{NH_3} + (1 - X_6) R_{H_2O}}{R_{gi}} \right) \dot{m}_9 \quad (15)$$

The energy balance for the evaporator is given by:

$$\dot{Q}_E = \dot{m}_9 (h_{10} - h_7) + \dot{m}_{gi} (h_{10gi} - h_{8gi}) \quad (16)$$

Liquid heat exchanger

The mass balance equations are:

$$\dot{m}_{11} = \dot{m}_1 \quad (17)$$

$$\dot{m}_8 = \dot{m}_3 + \dot{m}_5 \quad (18)$$

The energy equation is given by:

$$\dot{m}_3 h_3 + \dot{m}_5 h_5 - \dot{m}_8 h_8 = \dot{m}_1 (h_1 - h_{11}) \quad (19)$$

Absorber

The energy balance is expressed as:

$$\dot{Q}_A = \dot{m}_{10} h_{10} - \dot{m}_{11} h_{11} + \dot{m}_8 h_8 + \dot{m}_{gi} (h_{10gi} - h_{8gi}) \quad (20)$$

Coefficient of performance and circulation ratio

The COP is defined as the ratio between the refrigeration capacity and the heat transfer rate supplied by the generator:

$$COP = \frac{\dot{Q}_E}{\dot{Q}_G} \quad (21)$$

The circulation ratio is defined as the ratio between the mass flow rate of the strong solution that enters the generator and the flow rate of the refrigerant that goes to the evaporator. This quantity is expressed as:

$$f = \frac{\dot{m}_1}{\dot{m}_6} \quad (22)$$

Validation of the analytical model

Validation with models from the literature

The model developed in this work was validated by comparison with the model published by Starace and De Pascalis (2013). It is worth mentioning that in order to verify the consistency of the results, the present model was adapted to replicate the results obtained by Starace and De Pascalis (2013), when subjected to the same operation conditions, as shown in Table 1.

Table 1. Operation conditions adapted from the model of Starace and De Pascalis (2013)

Operation conditions	Value	Unit
Inlet temperature of the strong solution at the generator (T_1)	135	°C
Refrigerant vapor temperature after the rectification (T_6)	95	°C
Evaporation temperature (T_9)	-10	°C
Operation pressure (P)	25	bar
Heat source at the generator (\dot{Q}_G)	100	W
Same working fluids: ammonia, water and hydrogen		
The heat loss at the generator is neglected $\Rightarrow T_2 = T_3 = T_4$		

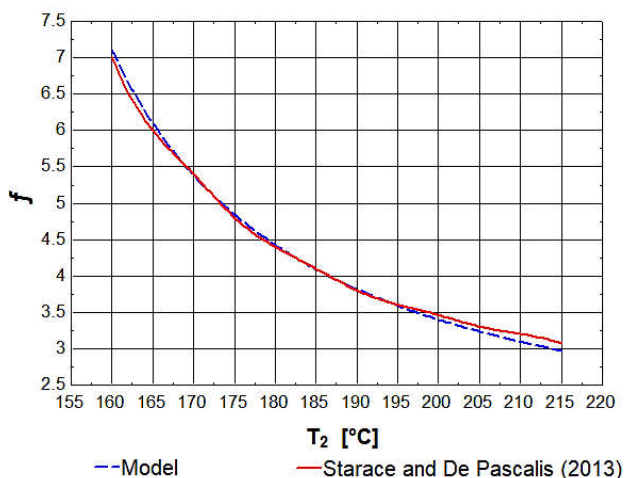


Fig. 2. Comparison of the results of circulation ratio versus the temperature of the generator from the present

Fig. 2 shows the results obtained by the presented model and the ones obtained by Starace and De Pascalis (2013). The maximum relative error is 3.34%. Despite the excellent results, it should be

mentioned that since the circulation ratio is dependent on the flow rates of the rich solution and the refrigerant produced, only the generator, bubble pump and rectifier influence the result. Thus, a further comparison is necessary to ensure that the model is reliable. It is important to state that the comparisons were made only by varying the generator temperature (T_2). Hence the other variables of the model are held constant, such as the heat source of the generator (\dot{Q}_G) and the outlet temperatures of the generator (T_3 and T_4). Fig. 3 shows the results of COP versus the temperature of the generator (T_2). It can be seen that, unlike the good agreement shown in Fig. 2, a significant disparity that continually increases as the temperature of the generator decreases is observed. It was obtained a maximum relative error of 16.2% between the results of the models within the range of temperatures considered.

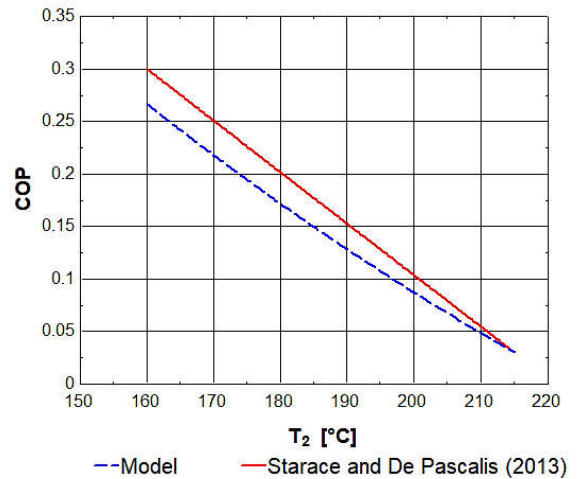


Fig. 3. Comparison of the results of COP versus the generator temperature between the present model and Starace and De Pascalis (2013)

It was found that when the temperature difference T_{8gi} minus T_8 is equal to 7.5°C ($T_{8gi} - T_8 = 7.5^\circ\text{C}$), the maximum relative error for the COP is 2.7%. In Fig. 4, the COP values versus generator temperature is presented.

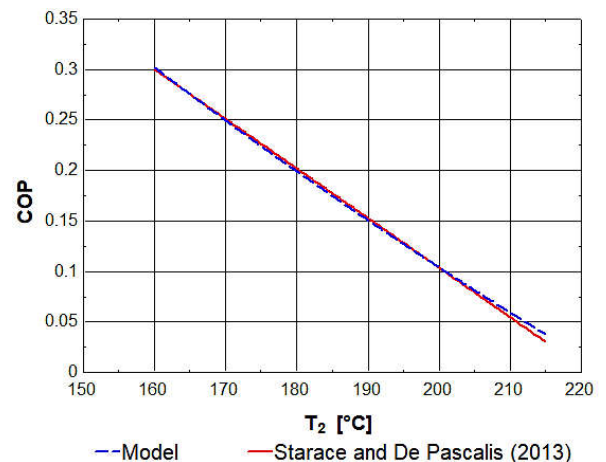


Fig. 4. Comparison between the results in the presented model and Starace and De Pascalis (2013) for the COP versus generator temperature after an increase in the temperature drop between points 8 and 8gi

Experimental validation: A small commercial DAR cycle refrigerator was used in order to verify the accuracy of the analytical model. Fig. 5 presents the experimental setup and the main points of interest. Before starting the experimental tests, the refrigerator was turned off for approximately two hours, in order to ensure thermal equilibrium with the environment. The $119 \pm 1.49 \Omega$ resistor used as the heating source in the generator works at 127 V, connected to the

electrical grid, where the voltage was measured. With a maximum observed variation of 2.5 V, the resistor dissipated an average power of 143.57 W, leading to a maximum variation of 5.49 W in the heat transfer rate to the refrigerator during the tests, as can be seen in Fig. 6.

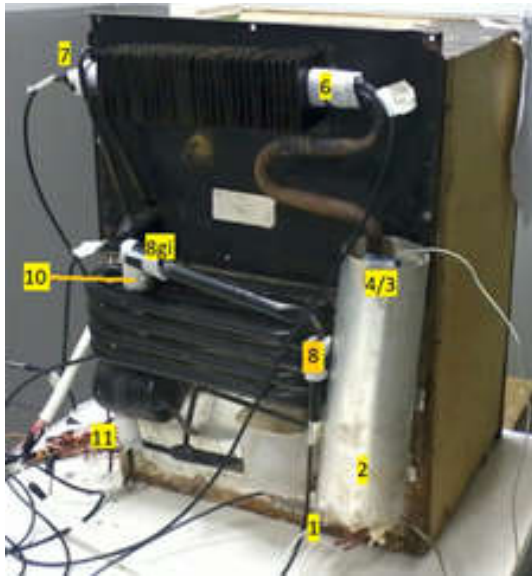


Fig. 5. Experimental setup

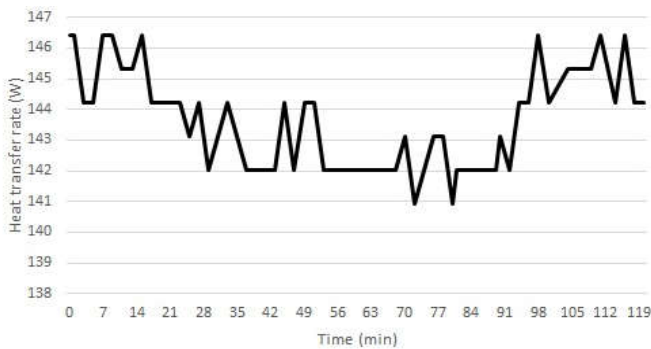


Fig. 6. Measured heat rate (Q_G) in the generator during the experimental tests

Figure 7 shows the temperature variation at the measured points of the refrigerator (see Fig. 5). The data acquisition system captured data every four seconds, generating 1,600 values for each sensors during the total period of test.

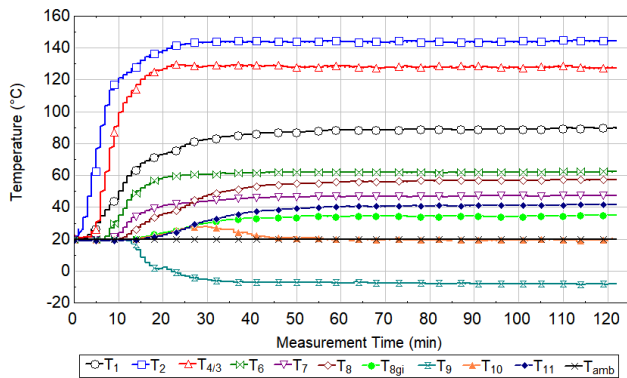


Fig. 7. Transient temperature measurements at the points of interest of the refrigerator

The model requires seven input data, including operating pressure, which was estimated from the condenser data. In this case, an external function available in the EES® software was used for determining ammonia-water mixtures properties. It is considered that the refrigerant enters the condenser as saturated vapor and leaves it as

saturated liquid. The temperatures used when comparing theoretical and experimental results were collected between 120 and 122 minutes of system operation, in which the maximum temperature fluctuation in the points did not exceed 0.5 °C. Within this time interval, the average heat rate in the generator was 144.21 ± 4.2 W and the operating pressure was 18.91 ± 0.25 bar. The input data for the analytical model are the temperatures at the points: 1, 2, 3, 4, 6, 9, the operating pressure and the heat rate of the generator. The temperature at point 7 was used to obtain the operating pressure. The properties at point 8 are computed considering the weak mixture is in the state of saturated liquid and that its concentration is the same as that in point 3. The third independent property at that point is the enthalpy, which is obtained considering that the LHE is isolated from the environment and calculated using Eq. 19.

As shown in the validation section, the temperature at the point 8gi was initially considered equal to the one at point 8. After the comparison with Starace and De Pascalis (2013), a temperature difference of 7.5 °C between these points ($T_{8gi} = T_8 - 7.5^\circ\text{C}$) was considered. Point 10 is calculated taking into account the saturated vapor with the same concentration as at point 9 ($X_6 = X_7 = X_9 = X_{10}$). Also, the partial pressure of the mixture with the H_2 is equal to the one at point 9. Finally, point 11 is determined taking into account that it has the same concentration as point 1, which is the state of saturated liquid at the same temperature as point 7. Table 2 shows the comparison between the analytical and experimental results.

Table 2. Comparison of the analytical and experimental results of the temperatures

Points	Analytical model (°C)	Experimental data (°C)	$\Delta\%$
1	89.6 ± 0.5	89.6 ± 0.5	0%
2	144.6 ± 1.5	144.6 ± 1.5	0%
3	127.9 ± 1.5	127.9 ± 1.5	0%
4	127.9 ± 1.5	127.9 ± 1.5	0%
5	127.9 ± 1.5	127.9 ± 1.5	0%
6	62.3 ± 0.5	62.3 ± 0.5	0%
7	47.3 ± 0.5	47.3 ± 0.5	0%
8	68.6 ± 1.11	57.1 ± 0.5	20%
8gi	61.1 ± 1.11	35.1 ± 0.5	74%
9	-8.3 ± 0.5	-8.3 ± 0.5	0%
10 and 10gi	21.5 ± 0.72	20.1 ± 0.5	7%
11	47.3 ± 0.5	41.6 ± 0.5	14%

The results on Table 2 show some considerable discrepancies for the temperatures at the points 8, 8gi, 11, 10 and 10gi. At point 8, the difference is explained by the hypothesis that the LHE is isolated. The results clearly show that there is a small heat exchange, which generated a temperature difference of 11.5 °C for the condition measured. This difference also affects the absorber's heat transfer rate computation. As the point 8gi, in the theoretical model, is dependent on point 8, the difference between the calculated value and the measured one also influence this result. However, with an even higher discrepancy (~26 °C). In addition, this affects directly the calculated COP, because the enthalpy of the H_2 (point 8gi) has a direct effect on the heat absorbed by the evaporator, as shown in Table 3.

Table 3. Comparison of the analytical and experimental results of heat transfer rates, COP and the circulation ratio

Results	Analytical model	Experimental data results	$\Delta\%$
\dot{Q}_A (W)	64.35 ± 2.7	72.78 ± 3.2	11.6%
\dot{Q}_R (W)	23.9 ± 1.8	23.9 ± 1.8	0%
\dot{Q}_C (W)	53.56 ± 2.4	53.56 ± 2.4	0%
\dot{Q}_E (W)	36.35 ± 1.7	46.63 ± 2.1	22%
\dot{Q}_P (W)	19.38 ± 2.2	19.38 ± 2.2	0%
\dot{Q}_G (W)	144.21 ± 4.2	144.21 ± 4.2	0%
\dot{Q}_{LHE} (W)	0	1.85 ± 0.67	100%
COP	0.252 ± 0.009	0.323 ± 0.011	22%
f	3.655 ± 0.111	3.655 ± 0.111	0%

The model operates under the hypothesis of a temperature drop of 7.5 °C between points 8 and 8gi. However, the measured data showed an even higher temperature drop (~22 °C). This difference indicates that it may not be possible to correlate these two points, as was performed in the models developed by Starace and De Pascalis (2013) and Zohar et al. (2005). Thus, new experimental tests were conducted to further investigate this issue. New experimental tests, namely tests 2 and 3 were carried out at lower and higher ambient temperatures, respectively. The remaining conditions are held the same as the prior tests. As in the experimental test 1, the average of the results obtained in the last minutes of the data collection was used for comparisons (see Table 4)

Table 4. Comparison of the average values used to collect the experimental data from the different tests

Points	Test 1	Test 2	Test 3	Uncertainty	Units
1	89.5	87.8	89.3	±0.5	°C
2	144.6	141.8	143.9	±1.5	°C
3 e 4	127.8	124.7	129.1	±1.5	°C
6	62.3	60.8	64.5	±0.5	°C
7	47.3	42.5	47.7	±0.5	°C
8	57.0	54.5	57.7	±0.5	°C
8gi	35.0	29.0	35.8	±0.5	°C
9	-8.2	-9.3	-7.0	±0.5	°C
10 and 10gi	20.0	17.5	23.3	±0.5	°C
11	41.5	38.0	40.8	±0.5	°C
T _{amb}	20.0	17.8	23.0	±0.5	°C
Q _G	144.21	144.21	139.84	±4.2	W
T ₈ - T _{8gi}	22.0	25.5	21.9	±0.5	°C
T ₇ - T _{8gi}	12.3	13.5	12.0	±0.5	°C
T ₇ - T ₁₁	5.8	4.5	7.0	±0.5	°C

The new tests show that, in fact, it is not possible to admit a direct dependence between points 8 and 8gi. Although test 3, with its highest ambient temperature, showed a quantitative agreement for the difference (T₈ - T_{8gi}), test 2 shows that lower ambient temperatures may increase this difference considerably. These observations suggest that the ambient temperature is the variable that most influences the temperature of point 8gi, the same form it influences the temperature of point 7 (condenser outlet). In this sense, also in Table 4, it is presented a comparison of the difference between these points, aiming to verify the possible relationship that would allow discarding the need to transform the temperature of point 8gi point into an input data. As can be seen, all tests showed a coherent relationship of about 12 °C between points 8gi and 7.

Model corrections based on experimental validation: In order to improve the model, some adaptations are made to the simplifying hypotheses. Starting with point 8gi, which will no longer be dependent on point 8, but point 7. Point 8 will become an input data allowing the LHE to be evaluated. Also, point 11 will remain related to point 7, however, with a minor correction.

In the refrigerator used in the experimental tests of this work, the correction hypotheses are:

- The temperature of the strong solution that leaves the reservoir (point 11) will be dependent on the temperature of the refrigerant that leaves the condenser (point 7), which, in this case, is cooled by ambient air. The order of magnitude will depend specifically on the refrigerator, which in the case of this work is $T_{11} = T_7 - 5$ °C;
- The temperature of the H₂ at the inlet of the GHE (point 8gi) will also be dependent on the heat exchange with the ambient air. Hence, it can be related to the temperature of the refrigerant at the outlet of the condenser (point 7). The order of magnitude will depend specifically on the refrigerator, in the case in question, $T_{8gi} = T_7 - 12$ °C;
- The temperature of the weak solution returning to the absorber (point 8) is now an input data, eliminating the hypothesis of an isolated liquid heat exchanger. In this case, Equation 19 is rewritten as:

$$\dot{m}_3 h_3 + \dot{m}_5 h_5 - \dot{m}_8 h_8 = \dot{m}_1 (h_1 - h_{11}) + \dot{Q}_{LHE} \quad (23)$$

With this procedure, as shown in Tables 5 and 6, the accuracy of the model increases considerably, thus being able to more accurately represent the behavior of a real refrigerator.

Table 5. Comparison of the analytical and experimental results of temperatures after adding the corrected hypotheses

Points	Analytical model (°C)	Experimental data (°C)	Δ%
1	89.55 ±0.5	89.55 ±0.5	0%
2	144.55 ±1.5	144.55 ±1.5	0%
3	127.85 ±1.5	127.85 ±1.5	0%
4	127.85 ±1.5	127.85 ±1.5	0%
5	127.85 ±1.5	127.85 ±1.5	0%
6	62.25 ±0.5	62.25 ±0.5	0%
7	47.25 ±0.5	47.25 ±0.5	0%
8	57.05 ±0.5	57.05 ±0.5	0%
8gi	35.25 ±0.5	35.05 ±0.5	0.6%
9	-8.25 ±0.5	-8.25 ±0.5	0%
10	21.45 ±0.72	20.05 ±0.5	7%
11	42.25 ±0.5	41.55 ±0.5	1.7%

Table 6. Comparison of the analytical and experimental results of heat transfer rates, COP and the circulation ratio after adding the corrected hypotheses

Results	Analytical model	Experimental result	Δ%
Q _A (W)	72.56 ±3.2	72.78 ±3.2	0.3%
Q _R (W)	23.9 ±1.8	23.9 ±1.8	0%
Q _C (W)	53.56 ±2.4	53.56 ±2.4	0%
Q _E (W)	47.02 ±2.1	46.63 ±2.1	0.8%
Q _B (W)	19.38 ±2.2	19.38 ±2.2	0%
Q _G (W)	144.21 ±4.2	144.21 ±4.2	0%
Q _{LHE} (W)	2.45 ±0.6	1.85 ±0.67	32.4%
COP	0.326 ±0.011	0.323 ±0.011	0.8%
f	3.655 ±0.111	3.655 ±0.111	0%

RESULTS AND DISCUSSION

As previously shown in Fig. 2, there is a direct reduction in the circulation ratio with the increase of the temperature of the generator. This is due, in large part, to the reduction in the flow of strong solution and, to a lesser extent, to the reduction in the flow of refrigerant. As the generator heat transfer rate (Q_G) and the generator's outlet temperatures (T₃ and T₄) remain constant in the current analysis, the mass flow rates decrease so that the overall energy balance is maintained. In addition, the reduction in refrigerant mass flow rate results, as shown in Fig. 3, in a decrease of the COP. This is explained by its dependence on the heat absorbed by the evaporator, which, in turn, is dependent on the mass flow rate of refrigerant produced in the generator. As the outlet temperature of the rectifier (T₆) increases, the purity of the ammonia in the refrigerant decreases, that is, there is an increase in the amount of water in the refrigerant. The more water there is in the refrigerant, the more difficult it will be for the condenser to reject the extra heat to the environment. Consequently, less ammonia will be condensed. In addition, excess water entering the evaporator may freeze, thus interrupting the operation of the system. Fig. 8 shows the influence of the rectifier temperature over the degree of rectification at different working pressures. In order to maintain high ammonia purity, the temperature at the outlet of the rectifier must remain below 70 °C. Fig. 9 presents the behavior of the COP versus the temperature the H₂, entering the GHE. The behavior observed could be explained by the fact the purpose of the hydrogen in the system is to cause the evaporation of ammonia in the refrigerator, generating the refrigerant non-equilibrium effect. The higher the temperature of the inert gas, the less useful heat will be absorbed by the ammonia, which, instead of absorbing heat from the cabinet, will heat up because of the inert gas. It can be noticed that an increase of 40 °C in the temperature resulted in a 28.4% reduction in the COP.

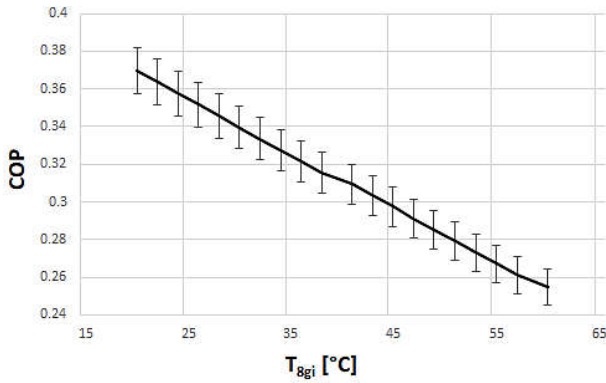


Fig. 9. Results of the COP versus the temperature at the point 8gi

This effect over the COP is not too severe, taking into account such a wide variation in temperature. This is explained by the fact that the contribution of the thermal capacitance of hydrogen is not as predominant as the ammonia. The condenser is one of the most important components in the system, as it is where the refrigerant condenses to be able to descend, by gravity, to the evaporator. Fig. 10 shows the results of COP versus the amount of saturated liquid produced during the operation.

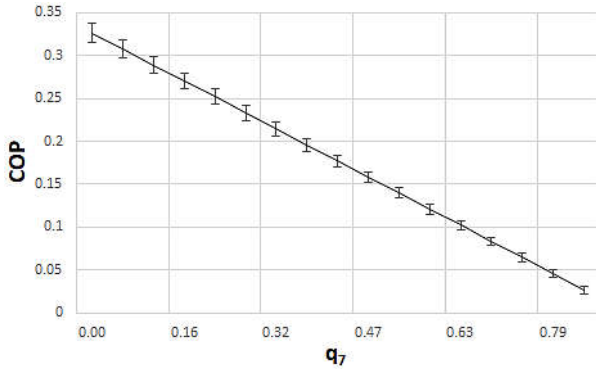


Fig. 10. Results of the COP versus the solution quality at the condenser outlet

The results shown in Fig. 10 were obtained taking into account the purity of 99.8% of ammonia in the solution. As can be seen, the production of condensate is vital to the system. With only half of the solution not condensing, the COP is reduced by 50%, due to the change in enthalpy, which affects the heat to be absorbed in the evaporator. It is noteworthy that this evaluation did not consider the deviation that allows excess vapor to escape to the absorber, which, if considered, would further increase the COP drop due to the decrease in the produced condensate mass flow rate. The temperature drop induced by H₂ in the refrigerant is the reason for its presence in the cycle and the order of magnitude of this drop will depend on the amount of H₂. Fig. 11 shows the behavior of the evaporator temperature with the mass flow rate of H₂.

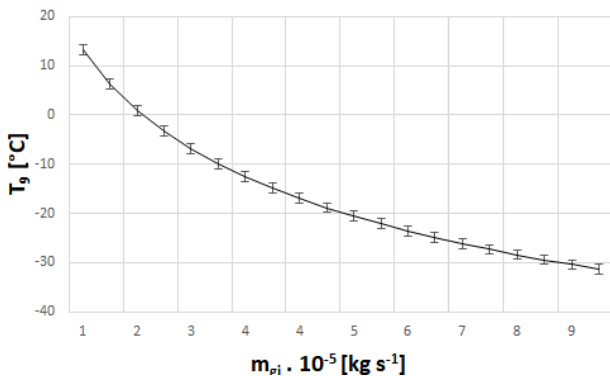


Fig. 11. Results of the evaporator temperature versus the hydrogen mass flow rate

As expected, as the amount of H₂ interacting with the liquid ammonia newly arrived at the evaporator increases, higher is the temperature drop due to the evaporation induced by the psychometrics imbalance. However, as can be inferred from Fig. 11, the necessity for a lower cooling temperature has other consequences. The Fig.12 shows the drop in COP with the increase in hydrogen mass flow rate.

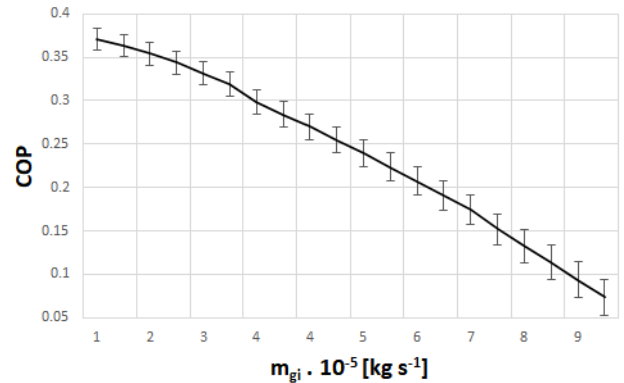


Fig. 12. Results of the COP versus the hydrogen mass flow rate

The COP is directly dependent on the evaporator capacity and its reduction is related to the lower heat transfer in the evaporator, as the hydrogen mass flow rate increases. This is explained by the fact that the ammonia will need to absorb more heat from the higher amount of hydrogen during its evaporation. This is associated with the negative effect of hydrogen, which adds an extra energy to be absorbed by the ammonia. The real consequence of this is that it will be necessary a longer time for cooling the cabinet. Therefore, it is important to address a kind of equilibrium for the evaporator temperature, so that the amount of inert gas required for this does not significantly affect the evaporator capacity.

CONCLUSIONS

A thermodynamic analytical model for a H₂O-NH₃-H₂ diffusion-absorption refrigeration (DAR) system was developed and its efficiency was analyzed for different simulation conditions. As demonstrated, the model is robust and its results are consistent when compared to data available in the referenced bibliography. The model validation was performed comparing the predictions of the theoretical model with the data collected experimentally. It was observed that some of the simplifying assumptions preliminary used in these works, as well as by other models in the literature, although useful for understanding the theoretical behavior of the cycle, proved inefficient in accurately describing the actual behavior of DAR refrigerator. Thus, a correction procedure was developed, which, after being tested, proved to be efficient in making the model more similar to the real system, which represents an important contribution for modeling and analyzing DAR systems. The purity of ammonia as a refrigerant after its rectification was also investigated as it represents an important parameter in the performance of the system. It was found that the higher the temperature at the outlet of the rectifier, the lower the purity of the ammonia. Therefore, to ensure less water flowing with ammonia, i.e., the high purity of the ammonia, the temperature at the outlet of the rectifier must be below 70 °C. It was verified that the temperature of the H₂ that goes to the GHE has a negligible impact on the COP, since the thermal capacitance of hydrogen is low when compared to the contribution of the ammonia enthalpy (energy) in the evaporator. The amount of saturated liquid produced in the condenser was evaluated and, differently from what was seen with the hydrogen temperature, it was observed that the COP is strongly affected by the quantity of condensate produced. For a 50% reduction in ammonia condensation, COP also reduces by 50%. This effect shows the importance of heat transfer by natural convection in this system. Finally, it was investigated how the temperature in the evaporator reduces due to the presence of the inert gas. It was found that the penalty for the operation at lower temperatures is a decrease in the

COP. The model proved to be robust in the operational conditions tested experimentally, but more tests under different operational considerations should be evaluated to improve the model's application range.

Acknowledgements: This study was financed in parts by the Coordenação de Aperfeiçoamento de Pessoal de Nível Superior - Brasil (CAPES) and the Brazilian National Council for Scientific and Technological Development (CNPq).

REFERENCES

- Adjibade, M. I. S., Thiam, A., Awanto, C., Azilinson, D. 2017. Experimental analysis of diffusion absorption refrigerator driven by electrical heater and engine exhaust gas. *Case Studies in Thermal Engineering*, 10(10), 255–261. <https://doi.org/10.1016/j.csite.2017.07.004>.
- Chen, J., Kim, K. J., Herold, K. E., (1996). Performance enhancement of a diffusion-absorption refrigerator. *International Journal of Refrigeration*, 19(3), 208–218.
- Holman, J. P., *Experimental Methods for Engineers*, eighth ed., McGraw Hill Publications, New York, 2012.
- Jelinek, M., Levy, A., Borde, I. (2016). The influence of the evaporator inlet conditions on the performance of a diffusion absorption refrigeration cycle. *Applied Thermal Engineering*, 99, 979–987. <https://doi.org/10.1016/j.applthermaleng.2016.01.152>.
- Mansouri, R., Bourouis, M., Bellagi, A. (2017). Experimental investigations and modelling of a small capacity diffusion-absorption refrigerator in dynamic mode. *Applied Thermal Engineering*, 113, 653–662. <https://doi.org/10.1016/j.applthermaleng.2016.11.078>.
- Mansouri, R., Mazouz S., Bourouis, M., Bellagi, A. (2015). Experimental study and steady-state modelling of a Commercial diffusion-absorption refrigerator. *Revue des Energies Renouvelables, Spécial ICT3-MENA*, Bou Ismail, 7–14.
- Mazouz, S., Mansouri, R., Bellagi, A. (2014). Experimental and thermodynamic investigation of an ammonia/water diffusion absorption machine. *International Journal of Refrigeration*, 45, 83–91. <https://doi.org/10.1016/j.ijrefrig.2014.06.002>.
- Rezende, T. T. G., Teixeira, F. N., Silva, J. A., Guimarães, L. G. M., Guzella, M. S. (2020). A non-intrusive method for evaluation ammonia mass flow rate in the condenser for diffusion-absorption refrigerators. *Flow Measurement and Instrumentation*, 72, 101695. <https://doi.org/10.1016/j.flowmeasinst.2020.101695>.
- Saâfi, I., Taieb, A., Salem, Y. B., Bellagi, A. (2019). Low capacity diffusion absorption refrigeration: Experiments and model assessment. *International Journal of Control, Energy and Electrical Engineering*, 9, 30–34.
- Santner, J., *Absorption Cooling*, Swarthmore College Engineering Department, 2009.
- Srikhirin, P., Aphornratana, S. (2002). Investigation of a diffusion absorption refrigerator. *Applied Thermal Engineering*, 22(11), 1181–1193. [https://doi.org/10.1016/S1359-4311\(02\)00049-2](https://doi.org/10.1016/S1359-4311(02)00049-2).
- Starace, G., De Pascalis, L. (2013). An enhanced model for the design of Diffusion Absorption Refrigerators. *International Journal of Refrigeration*, 36(5), 1495–1503. <https://doi.org/10.1016/j.ijrefrig.2013.02.016>.
- Von Platen, B.C., Munters, C.G., 1928. Refrigerator. US Patent#, 1,685,764.
- Zohar, A., Jelinek, M., Levy, A., Borde, I. (2005). Numerical investigation of a diffusion absorption refrigeration cycle. *International Journal of Refrigeration*, 28(4), 515–525. <https://doi.org/10.1016/j.ijrefrig.2004.11.003>.
- Zohar, A., Jelinek, M., Levy, A., Borde, I. (2009). Performance of diffusion absorption refrigeration cycle with organic working fluids. *International Journal of Refrigeration*, 32(6), 1241–1246. <https://doi.org/10.1016/j.ijrefrig.2009.01.010>.
